

The effects of ICRF heating on plasma edge conditions in PLT

P. L. Colestock, S. A. Cohen, J. C. Hosea, D. Q. Hwang, G. J. Greene, J. R. Wilson, M. Ono, D. Manos, R. Budny, G. Hammett, and R. Kaita

Citation: *Journal of Vacuum Science & Technology A* **3**, 1211 (1985); doi: 10.1116/1.573066

View online: <http://dx.doi.org/10.1116/1.573066>

View Table of Contents: <http://scitation.aip.org/content/avs/journal/jvsta/3/3?ver=pdfcov>

Published by the AVS: Science & Technology of Materials, Interfaces, and Processing

Articles you may be interested in

[Edge measurements during ICRF heating in PLT](#)

AIP Conf. Proc. **159**, 274 (1987); 10.1063/1.36693

[ICRF heating in fusion plasmas](#)

AIP Conf. Proc. **159**, 211 (1987); 10.1063/1.36679

[ICRF coupling with a ridged waveguide on PLT](#)

AIP Conf. Proc. **159**, 322 (1987); 10.1063/1.36625

[ICRF heating experiments on the PLT tokamak](#)

AIP Conf. Proc. **129**, 28 (1985); 10.1063/1.35270

[Deuterium flux measurements in the edge plasmas of PLT and PDX during auxiliary heating experiments](#)

J. Vac. Sci. Technol. **20**, 1234 (1982); 10.1116/1.571550



A PASSION FOR PERFECTION

PFEIFFER VACUUM

ACP dry, multi-stage Roots pumps

- Reliable clean vacuum with lower operating costs
- Two years between maintenance
- Models from 15 to 40 m³/h

Are you looking for a perfect vacuum solution?
Please contact us!

The effects of ICRF heating on plasma edge conditions in PLT

P. L. Colestock, S. A. Cohen, J. C. Hosea, D. Q. Hwang, G. J. Greene, J. R. Wilson, M. Ono, D. Manos, R. Budny, G. Hammett, and R. Kaita
Plasma Physics Laboratory, Princeton University, Princeton, New Jersey 08544

(Received 24 September 1984; accepted 28 January 1985)

The interaction of ICRF heating with the plasma edge in Princeton large torus (PLT) is reviewed and possible mechanisms responsible for the observations are discussed. Ion and neutral sputtering are found to be the most significant producers of impurities, which are observed to increase in moderate amounts during ICRF heating. Collisional edge heating by the rf is evaluated as a possible explanation of measured electron density increases and particle fluxes. Antenna conditioning is also discussed, relating to the processing necessary to achieve the highest power handling capability per antenna in PLT.

I. INTRODUCTION

Significant progress has been made in recent years toward the realization of rf heating methods capable of bringing tokamak devices close to a thermonuclear plasma parameter regime.¹ In particular, heating by means of rf power coupled near the ion cyclotron frequency of a plasma ion constituent (coined ion cyclotron range of frequency or ICRF) has produced efficient plasma heating in a number of experiments worldwide.^{2,3} Along with the heating, a number of side effects upon the heated plasma have been observed which, if not controlled, could limit the usefulness of rf heating in reactor-sized devices. Perhaps the most important of these effects is an increase in the plasma impurity content proportional to the applied rf power.^{1,2} Such an impurity increase enhances bremsstrahlung and recombination line radiation losses and depletes the reacting hydrogenic ion species. In order to understand and control the rf-induced impurity influx as well as the other side effects, much experimental attention has been focused on determining the source of the impurities and the scaling of the impurity influx with plasma parameters. The focal point of this study is the optimization of the rf antenna to maximize power handling capability while controlling any deleterious rf-induced side effects.

In this paper, we examine the existing body of experimental data related to impurity generation (Sec. II). In Sec. III, we discuss possible mechanisms responsible for the observations and in Sec. IV, we summarize and draw the conclusions of this work.

II. EXPERIMENTAL RESULTS

A. Antenna conditioning

In ICRF heating experiments, the rf power is most commonly inductively coupled to the plasma with strip lines or loops, as shown schematically in Fig. 1. The power matching circuit is configured so that the rf current is maximum in the center of the loop at the midplane. Since the power radiated into the plasma is proportional to I^2 , most of the power is radiated from the outside midplane for the low field side antennas in use on PLT. The impedance presented by the plasma is normally much lower than the characteristic impedance of the loop, so that a standing wave builds up on the antenna with a Q of 10–20. The consequence of this standing wave is a decrease in the rf current away from the midplane,

accompanied by an increase in the rf voltage. It was observed early in the ICRF heating program that direct contact between the loop antenna and the plasma led to power losses which reduced the overall heating efficiency.⁴ Thus a metallic shield, the so-called Faraday shield, was installed in front of the loop to screen the antenna from the edge particle flux while permitting good inductive coupling to the plasma. A second function of the shield was to eliminate stray rf electrostatic fields parallel to the magnetic field lines so as to eliminate possible surface wave generation or coupling into nonpenetrating dissipative mechanisms. The result of this step was a significant increase in heating efficiency, and it has led to the widespread adoption of the Faraday shield concept in ICRF antenna design. While primarily a benefit to low power experiments, the Faraday shield has come under increasing scrutiny as a possible source of impurities as the rf and plasma heat loading of the shield elements becomes more severe in present day experiments. Efforts have been concentrated on limiting the damage to the shield elements and the consequent release of impurities to the plasma. For inductive coupling, the dilemma is faced that, to

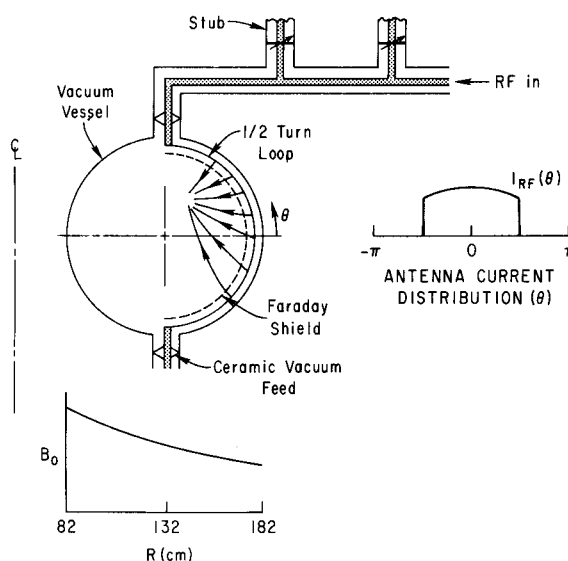


FIG. 1. Schematic of an ICRF one-half-turn loop antenna. A standing wave developed in the antenna provides a current distribution as shown in the inset. The frequency is adjusted to match the resonant cyclotron frequency of an ion on the centerline of the cross section.

minimize shield damage, the antenna shield should be well behind the face of the limiter in the plasma scrapeoff region, while at the same time the antenna coupling to the plasma is weakened, increasing the antenna voltage and stored rf energy. While these problems have proved to be manageable in current devices, future requirements require development of antennas capable of withstanding long pulse, high thermal loading conditions.

During operation of these antennas, a dramatic increase in the power handling capability occurs after installation during a breaking-in period which includes both vacuum and plasma conditioning. Before installation each element is cleaned and baked in air at 120 °C for 3–6 h to remove excess water and absorbed gases. After the initial pump down, the antennas are rf cleaned by first applying a series of 1–5 ms pulses at increasing rf powers until normal operating voltages are reached with no release of gas during the rf pulse. The antennas are pulsed in vacuum with no applied magnetic field. During this phase, rf breakdown often occurs on the antenna creating a low-density glow which aids in cleaning the antenna surfaces. As will be discussed further, Faraday shield strips of stainless steel have been used in experiments on PLT. These strips have been installed bare or with cladding of titanium or graphite. Of these, the stainless-steel shields exhibit a nonreversible improvement in power handling of 10–20 times the initial operating levels. The other materials tested require periodic reconditioning to drive out accumulated gases. After the initial period of conditioning, the rf pulses are lengthened until all breakdown has ceased at normal pulse lengths, 0.1–0.3 s. At this time the antennas are used in full discharge operation during which further improvement is observed over the course of 100–200 discharges. Still longer term improvements in rf operation are observed on the scale of 2000–5000 discharges which are thought to be related to long-term changes in the PLT device itself (wall and limiters). It is worthwhile to note that the number of discharges required to reach optimum power handling capability can be significantly reduced by the use of titanium gettering. In this process, a layer of titanium is deposited directly on the Faraday shields and nearby vessel walls by heated titanium balls which are inserted into the vacuum vessel between discharge pulses. An improvement in the antenna power handling capability of up to 100% is observed depending on prior antenna conditions. Also associated with the titanium gettering is an improvement in the discharge stability and operating range believed to be due, in part, to a reduction of oxygen in the discharge by the gettering action of the titanium.

Also important in these studies is the location and the relationship of the limiters to the antennas. It was observed in PLT that limiters placed close to the antennas resulted in abnormally low voltage breakdown on the antenna. A similar effect was observed when a gas feed was located close to the antenna, and was believed to be due to the buildup of neutrals in and near the antenna elements.

B. ICRF heating results

During high-power ICRF heating, an increase in the line-average electron and hydrogenic ion density is observed, as

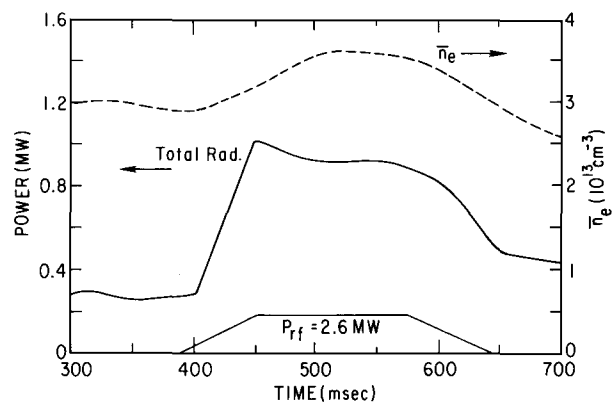


FIG. 2. Line-average electron density and total radiated power for an applied rf power of 2.6 MW. The fraction of the total applied power lost by radiation is approximately the same for both the Ohmic- and rf-heated plasmas.

shown in Fig. 2. The magnitude of this increase depends on rf power, plasma conditions, and previous discharge history. The density rise has been measured spectroscopically to be primarily due to hydrogenic ion species. However, under poor wave absorption conditions and at the highest applied rf powers, a significant part of the density rise may be due to carbon and oxygen (metallic impurities also increase but do not significantly displace hydrogenic species in the plasma).⁶ It is worthwhile to note that the ion densities are inferred from visible, x-ray spectroscopy, charge exchange, and neutron emission measurements. While absolute densities are difficult to ascertain, it is believed that relative changes can be determined relatively accurately ($\leq 5\%$). For given plasma conditions, the density increase appears to be at a minimum for the strongest wave absorption (Fig. 3). In the case of a ^3He minority ion species in a predominantly deuterium background plasma, the wave absorption is maximum when the ^3He ion concentration is about 5%–7% of the total density. A similar weak minimum in the density increase is observed when the ion-cyclotron resonance for ^3He is positioned on the axis of the device, again corresponding to

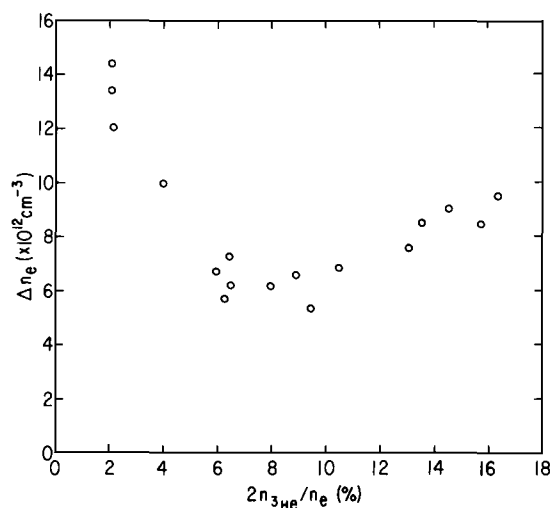


FIG. 3. Line-average electron density increase as a function of ^3He content in a deuterium background plasma. $P_{rf} = 500$ kW. Maximum absorption is predicted theoretically to occur in the range of 5%–10% ^3He (Ref. 5).

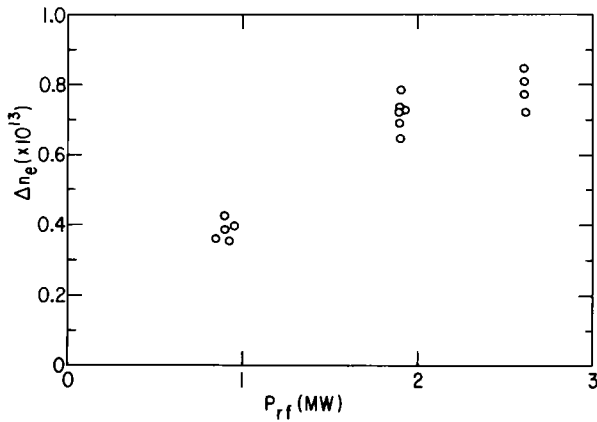


FIG. 4. Electron density increase as a function of applied rf power in a D- ^3He plasma. In these experiments the initial density, plasma current gas flow, and toroidal field were held constant ($I_p = 450$ kA, $n_{ei} = 1.8 \times 10^{13}$ cm $^{-3}$).

maximum absorption. It is also observed that the density increment is proportional to the rf power but saturates at high powers, as shown in Fig. 4. Moreover, this increase depends on whether or not the walls (and antennas) have recently been coated with gas and whether titanium gettering has been applied. Along with the density increase, a strong increase in the low-energy edge neutral efflux⁷ is observed, as shown in Fig. 5. These results suggest that a reservoir of loosely bound hydrogenic gas is freed by the rf heating and enters the plasma scrapeoff region, increasing the recycling and the flow of neutral gas into the plasma core. The increase is apparently toroidally symmetric, as evidenced by the similar flux enhancement observed close to and far from the limiters.

The power reaching the plasma surface associated with the rf heating is in the form of radiation and charged-particle and neutral fluxes. The charged-particle flux measured bolometrically⁸ shows specific pitch angle information, which reflects the nature of the heating mechanism, as shown in

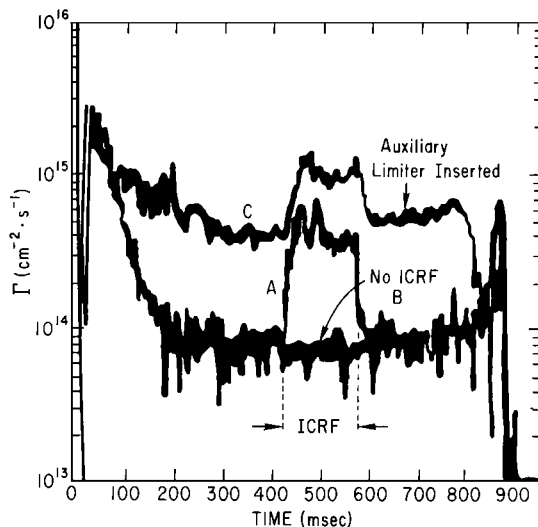


FIG. 5. Charge exchange D^0 efflux as a function of time for three cases during ICRF heating of a D- ^3He plasma with $P_{rf} \sim 1$ MW. The flux is integrated over the energy range 25–1000 eV. A and B are observations away from the limiters. C shows observations near an auxiliary limiter.

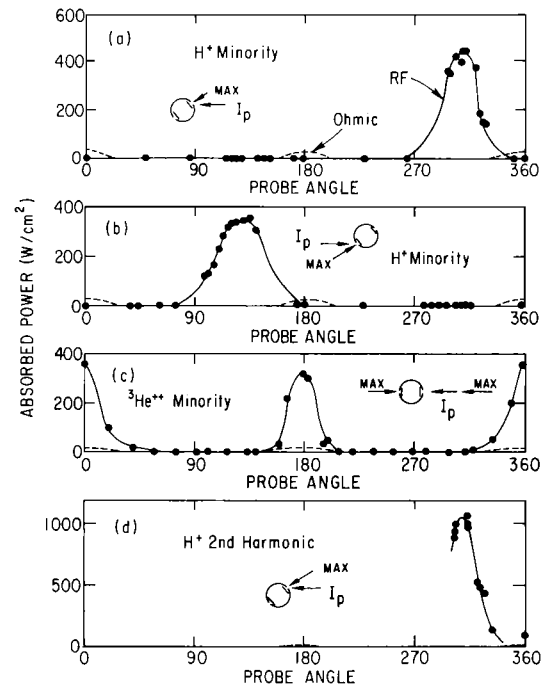


FIG. 6. (a) Heat flux to bolometric probe (shown schematically) as a function of rotation angle relative to plasma current; D $^+$ plasma with H $^+$ minority with $P_{rf} \sim 1$ MW. (b) Same as (a) with all fields and I_p reversed. (c) Same as (a) for $^3\text{He}^+$ minority with $P_{rf} \sim 1.5$ MW. (d) Same as (a) for H $^+$ second harmonic with $P_{rf} \sim 2$ MW.

Fig. 6. These probe measurements indicate a significant flux of suprathermal ions with pitch angles $V_{\perp}/V_{\parallel} \sim 1.6$ received at the outside midplane for the cases where hydrogen ions are resonantly heated by the rf. On the other hand, no such flux has been observed in ^3He resonance heating situations under similar discharge conditions and no fast particles have been observed at all with probes located at the top of torus. These results are qualitatively explained by the tendency of the ICRF to generate resonant fast-ion distributions, as shown by charge exchange measurements in Fig. 7. The rf accelerates the resonant ions in the perpendicular direction and for sufficiently weak collisionality, e.g., high energy, will cause velocity space diffusion, which tends to cause an accumulation of trapped particles with their turning points on the resonance layer.⁹ The pitch angle at which the maximum probe signal occurs, i.e., $V_{\perp}/V_{\parallel} \sim 1.6$, shown in Figs. 6(a), 6(b), and 6(d), corresponds to the trapped ion orbit having its turning point on the resonance layer and its midplane intercept at the probe location, i.e., $V_{\perp}/V_{\parallel} \sim 1.6$. The absence of ^3He flux at this pitch angle is consistent with a fast-ion density for ^3He that is expected to be ~ 200 times less than the H density for similar discharge conditions, owing to the stronger collisional coupling of ^3He to the bulk ions.¹⁰ Further evidence for the identification of the ion flux as rf generated has been gleaned from the dependence of the flux on resonant ion density. As the hydrogen density was increased by gas puffing during the rf, the H efflux showed a precipitous drop, consistent with the exponential dependence of the tail temperature on resonant ion density. Based on this model, some information as to the rf deposition profile can be deduced from the results shown in Fig. 8. Here, the resonance layer location was varied by changing the toroidal field,

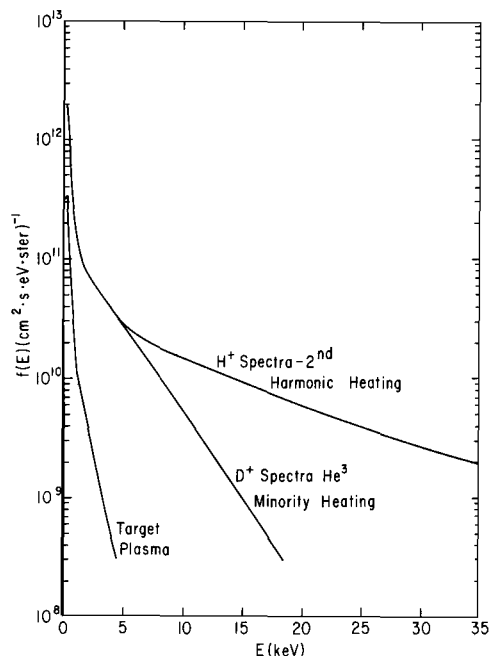


FIG. 7. Charge exchange flux spectra in PLT for Ohmically and ICRF-heated plasmas with $P_{rf} \sim 1$ MW. Although not shown, minority heating of H^+ and 3He also produce energetic ion tails.

while the bolometric probe measured the ion flux at the peak flux pitch angle. As the resonance layer moves inward from the wall, the ion flux rises, due to the increased numbers of observable resonant ions able to sample the resonance layer. As the layer moves further inward, a drop in the measured flux suggests that the rf deposition profile moves inward away from the observable top and bottom regions of the discharge. These results are consistent with a deposition profile

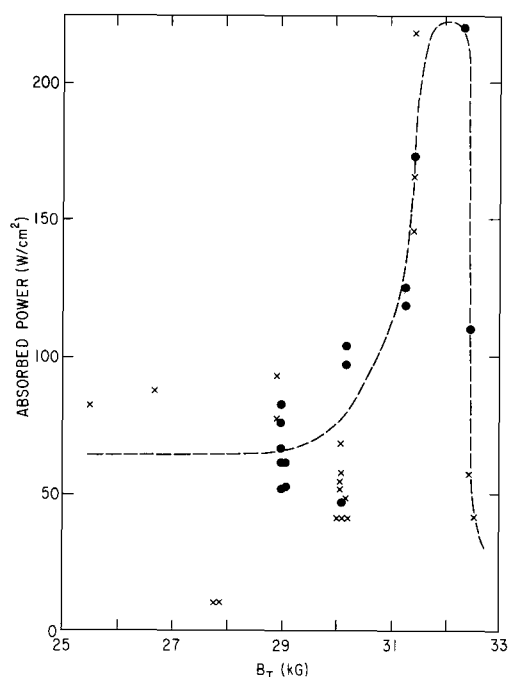


FIG. 8. Total heat flux of co-going particles vs toroidal magnetic field. The probe was stationary at $R = 173$ cm. This variation of field moves the H^+ resonance layer from 119 (25 kG) to 158 cm (33 kG). \bullet ~ 980 kW; \times ~ 660 kW.

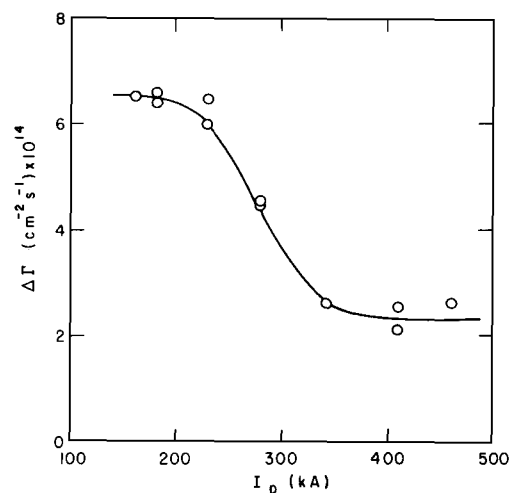


FIG. 9. Edge neutral efflux increase as a function of plasma current as deduced from charge exchange measurements with $P_{rf} \approx 200$ kW (20–1000 eV).

that is predominately within the inner 20 cm. A consequence of the production of ion tails is that the efficiency of the rf depends on the ability of a given fusion device to confine these fast ions in the plasma core. The importance of good fast-ion confinement was demonstrated by a scan of the plasma current during rf heating in PLT. Since the fast-ion confinement improves with increasing I_p ,¹¹ the best heating results are obtained at sufficiently high current. Depicted in Fig. 9 is a decrease in the low-energy (20–1000 eV) neutral efflux associated with the highest efficiency heating conditions (i.e., high current).

In related measurements it has been observed that an increase in both low-Z (O, C) and high-Z (Ti, Fe) impurities occurs during ICRF heating.¹¹ This is evidenced by an increase of selective line radiation from these elements, as well as from an increase of bremsstrahlung radiation. It is interesting to note that while the total radiated power increases by 3 times during the rf, the radiated fraction of the total applied power remains the same, as in the Ohmic heated case. Nonetheless, the presence of impurities causes a depletion of the reacting hydrogenic species in the core, and it would be desirable to limit their influx. In order to fully understand the origin of impurities, the Faraday shield material, as well as the antenna configuration, was varied. A comparison of Faraday shields was made using either titanium or stainless-steel shields,⁶ as shown in Fig. 10. These results indicate that the heavy ion content depends on the choice of Faraday shield material. The heavy impurity density has been found to increase nearly linearly with rf power up to ~ 3.0 MW, applied thus far in PLT. In another experiment, poloidally short antennas were used to determine whether or not the ion cyclotron resonance near the antenna (top and bottom locations) at the surface could lead to enhanced impurity production. The results, shown in Fig. 11, indicate that no significantly different impurity densities were observed under similar discharge conditions for the two types of antennas. Nor was the heating efficiency of either antenna measurably different. Light impurities, particularly C, also increase during rf and are estimated to account for most of

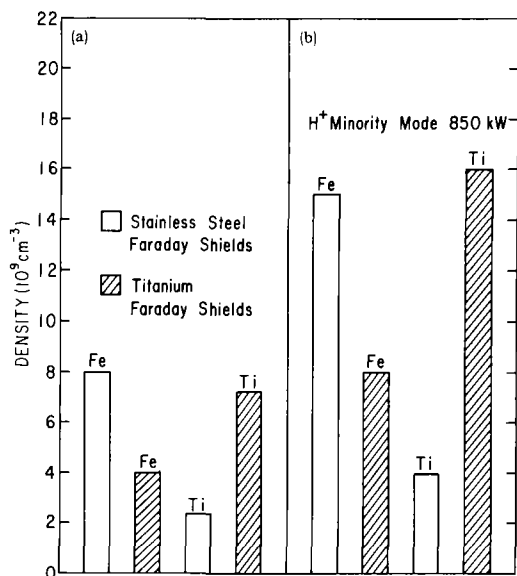


FIG. 10. Comparison of the total titanium and iron densities (a) before and (b) during ICRF heating in PLT. As indicated, the antenna had either titanium or stainless-steel Faraday shields.

the hydrogenic ion depletion. These originate chiefly from the limiters, since they are the primary source of carbon in contact with the plasma. The level of increase does not appear to depend on the proximity of the limiters to the antenna. Qualitatively, these results agree with those from other ICRF experiments; however, the impurity levels observed

in PLT are usually lower than in these other devices.^{2,3} The reasons for this difference are believed to be due to the larger plasma current normally used in PLT, as well as the comparatively larger plasma size, which helps to insulate the walls from the plasma core. It is expected that this favorable size scaling will continue to larger devices, further reducing the problem of plasma impurity contamination associated with rf heating.

It is also instructive to examine the failure modes of the rf heating. During the early phases of antenna conditioning, the gas emitted from the antennas can lead to plasma disruptions through sudden changes in the current profiles. Such changes typically take the form of edge electron cooling on a time scale of 20–50 ms. Also, arcing on the antenna elements can occur, which releases a sudden burst of Faraday shield material into the discharge by means of localized melting of the shields. As the antennas become conditioned, this arcing occurs at progressively higher rf powers, but remains the ultimate limit of antenna power handling capability. To date, power flux levels of $\sim 1 \text{ kW/cm}^2$ of antenna surface area have been achieved on PLT. Under high-power operating conditions, the presence of an rf-sustained glow discharge about the antenna or rf power feeds has also been detected. The rf glow consumes a portion of the rf power ($< 10\%$) for sustaining the glow plasma, which is quickly lost to the walls and antenna elements. It is believed that this loss can be a deleterious drain on the coupled rf power, as well as an additional surface heating mechanism in the vicinity of the antenna. This glow has been suppressed partially by a redesign of high electric-field stress components but may remain a problem at the highest achieved power levels.

III. DISCUSSION OF EDGE HEATING MECHANISMS

There are at least two ways in which the rf can deposit power in the edge plasma: by collisional heating of scrapeoff particles and by joule heating of surfaces. In addition to these mechanisms, a pronounced increase in the edge power efflux is to be expected as a consequence of the substantial amounts of applied auxiliary power. As already discussed, edge losses may occur as an enhancement of thermal particle flows, as well as from rf-induced fast-ion losses. Such changes in the edge parameters can lead to the observed density increase and impurity influx by several microscopic processes including evaporation, desorption, ion sputtering, charge exchange neutral sputtering, and arcing. Evaporation can occur as localized hot spots which are created by either particle bombardment or joule heating, and is most severe on the Faraday shield elements. For present conditions, it is estimated that a maximum of about 40 W/cm^2 is dissipated on each shield element by joule heating, which should only result in a temperature rise of a few degrees during each pulse. Although future long-pulse systems may need to invoke active cooling of shield elements, joule heating is not likely to be a source of impurities in present experiments. On the other hand, antenna damage has been observed and attributed to severe particle bombardment, possibly during disruptions. This damage was not caused by the rf power, but the close proximity of the antenna to the plasma which was needed for good rf coupling. This makes

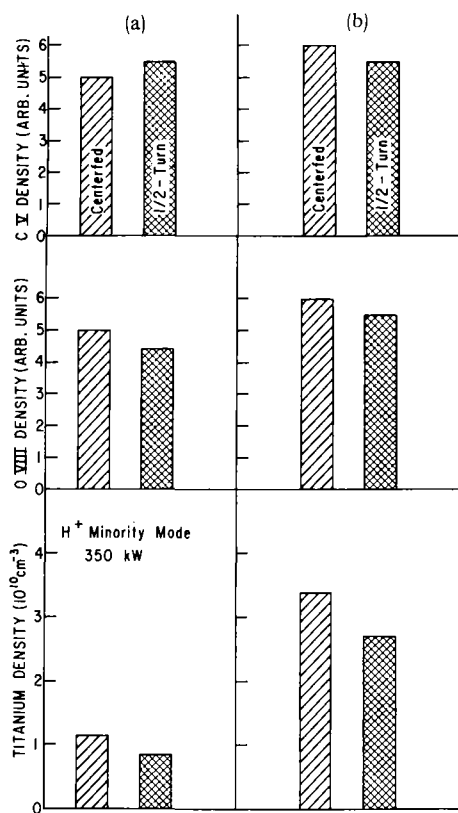


FIG. 11. Comparison of impurity densities for equal powers from either a one-half-turn loop antenna or a poloidally short (60°) center-fed antenna, for (a) before and (b) during ICRF. The antennas had roughly equal areas and showed no significant differences in impurity contamination.

the shield elements vulnerable to particle bombardment. The longevity of the shields has been extended by the installation of graphite protective fingers near the observed damage locations. Ion sputtering occurs on the limiters and over all surfaces near the limiter scrapeoff radius. The ions impact with an energy equal to their kinetic energy plus Z times the sheath potential, which is a few times T_e (at $r = 40$ cm). In PLT, the ion population is typically comprised of thermal metallic impurities ($\sim 0.1\%$), thermal low- Z impurities (C, O) ($\sim 1\%$), suprathermal rf-accelerated hydrogenic ions ($\sim 0.01\%$), and thermal hydrogenic ions. Of these classes, the thermal hydrogenic ions alone are able to cause the limiter and shield sputtering observed. The level of sputtering is a sensitive function of the edge electron temperature, which determines the sheath potential. In addition, sputtering may be aided by the presence of the small number of suprathermal ions. In PLT, the rf-induced fast ions are most easily lost to the walls near the pitch angles associated with trapped resonant ions, as discussed earlier. Upon entering the loss cones, these fast ions impact the vessel walls and loosen the surface atoms, which in turn may be more effectively sputtered by thermal ion population.¹² Alternatively, the preferential loss of rf-induced fast ions may cause the plasma to charge relative to the vessel, thereby increasing the sheath voltage drop and consequent ion sputtering. At present, there is not enough experimental information available to ascertain the precise role of fast-ion losses in impurity generation. Another possibility for explaining an rf-induced enhancement of sputtering is direct edge electron heating. If even a small amount of the rf power is lost in the surface, the resulting electron temperature rise there can significantly enhance the surface sputtering. This fact is consistent with the observation that reduced central core wave damping increases the rf power available for edge heating, causing both an impurity influx and larger density rise. To estimate the level of rf power deposited in the surface, the induced wave fields are calculated, including the effects of edge collisionality and a localized antenna.¹³ This calculation is performed for the case of the ion-cyclotron resonance layer on the axis passing near the ends of the antenna at the top and bottom of the plasma. The wave energy is radiated from the antenna and propagates radially inward, where it is partially absorbed, reflected, and transmitted at the resonance layer. In this model, the absorptivity and reflectivity of the central region result in a partial standing wave between the resonance layer and the antenna. Of importance for the edge heating is that the field energy density near the antenna is roughly four times that of the core, due to the near-zone antenna fields. The poloidal electric field strength contours are shown in Fig. 12 for a typical PLT case. Collisionality is included in the calculation, according to Ref. 14, and the results indicate that 0.5%–1% of the rf power can be lost near the edge, mainly through electron–ion collisions. Although small, this level of power deposited in the antenna near field is adequate to account for the observed increases in edge density and temperature. Since the applied rf power is five to six times the Ohmic power, a few percent of the rf power deposited at the edge still represents a two to five fold increase over Ohmic heating of the power flowing into the

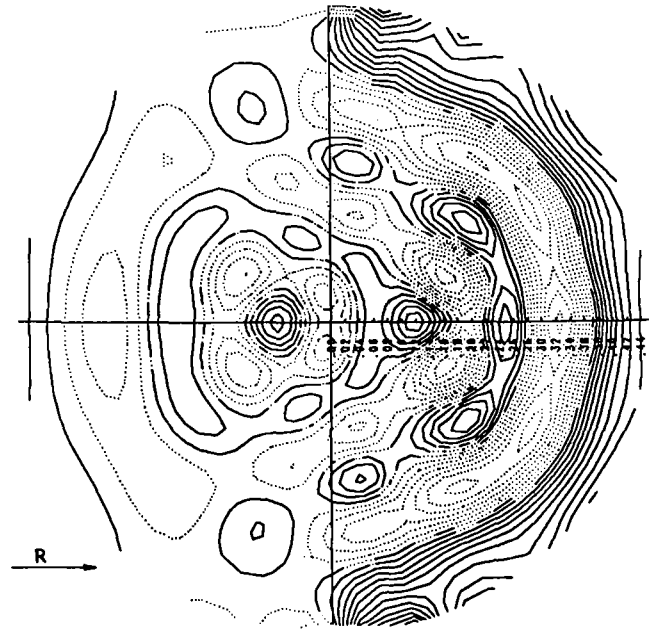


FIG. 12. Theoretical calculation of wave magnetic field strength contours in the antenna plane for the D-H heating case in PLT. Strong absorption by H^+ in the plasma core depletes the wave energy but a small amount of collisional edge damping may also occur in the strong near field of the antenna.

edge region. If the edge confinement is not altered appreciably, then this level of edge power increase is consistent with the observed density and electron temperature increases. The strong fields that occur near the antenna are due to the nonpropagating part of the broad wave spectrum excited by a finite-sized antenna. It is conceivable according to this model, that an appropriately phased array of antennas could be made to minimize the strong surface fields but still allow good coupling to the bulk plasma. The experimental data gathered thus far with phased antenna pair in PLT is inconclusive; however, recent Japanese results¹⁵ indicate that appropriate antenna phasing can reduce the impurity influx by a factor of 2.

Other candidates for edge heating include electrostatic wave generation and absorption, and possible rectification of the rf in the sheath at the wall. In the former, recent measurements and theoretical work have shown that electrostatic Bernstein waves may be directly generated even by Faraday-shielded antennas through the action of edge density gradients on the coupling.¹⁶ Although the fate of this wave energy has not been established experimentally, theoretical calculations indicated the power lost in the surface should remain small. Experiments are currently underway to test this conclusion. In the case of sheath rectification, additional power could be dissipated if the rf causes the plasma potential relative to the wall to increase up to an appreciable fraction of the rf electric field amplitude. For the scrapeoff parameters during rf heating in PLT ($n_e \sim 10^{11} \text{ cm}^{-3}$, $T_e \sim T_i \sim 10 \text{ eV}$), we estimate $\sim 0.5 V \text{ W/cm}^2/V$ can be deposited on surfaces intersecting field lines, where V is the effective sheath voltage drop in volts. The effective voltage drop is that which occurs across the sheath in the presence of the rectified rf power. Over much of the vessel, this level is much smaller than other

power loss mechanisms, such as charge exchange and radiation. Near the antennas, however, the voltages could be several hundred volts in present experiments, making this mechanism the dominant loss process locally. Further experimental information is required to clarify this situation.

In addition to the above mechanisms, the observed enhance neutral efflux can be responsible for a significant amount of the rf-induced impurity increase by neutral sputtering of walls and limiters. Estimates of the sputtering due to measured neutral fluxes can account, within a factor of 2, for the increase in metallic impurities from the walls.⁷ This neutral efflux, and the resulting sputtering, is a consequence of auxilliary heating in PLT, and is not restricted to ICRF heating. The precise nature of the mechanism which enhances particle recycling, and consequently neutral efflux at the edge in the presence of rf, is not well understood. It is likely that the edge electron heating described earlier plays a role in this process, but other factors include the modification of the sheath potential and fast-particle bombardment. The understanding and control of particle recycling at the edge is currently an active area of research. Efforts are underway to reduce the edge neutral flux in PLT, thereby reducing neutral sputtering and possibly the electron density increase.

A final mechanism which can lead to impurity generation is arcing. While the detailed surface physics associated with an rf-induced arc is not well understood, it is likely that localized melting and evaporation of the Faraday shield material can occur, releasing large quantities of impurities into the plasma. However, as the antennas become conditioned, rf-induced arcing ceases to be a problem and does not need to be considered as a factor during normal operation. Nonetheless, attention in the antenna design should be given to reducing the conditioning process by minimizing high field-stress points where possible.

IV. SUMMARY AND CONCLUSIONS

Recent experimental results have shown that effective rf heating of tokamak plasmas can be achieved at powers up to 5–6 times Ohmic levels. The trend to larger, higher current machines with good fast-ion confinement is partially responsible for the success of ICRF heating in the current generation of devices. Along with this heating, an increase in the

plasma density and purity content is experienced. These phenomena are likely due to the small edge power deposited by the rf, to fast-ion losses, and to the global increase of the plasma energy content. The structures which produce the impurities are the limiters and Faraday shields by ion sputtering, and the entire walls by neutral sputtering. The trend to larger devices should reduce these effects by reducing the surface-to-volume ratio and increasing wall-to-plasma distances. The use of divertors instead of limiters may further reduce impurity levels, although the antennas must still remain close enough to the plasma to ensure good rf coupling. There is a need for the development of antenna designs which are hardened to particle bombardment without the sacrifice of power handling capability.

ACKNOWLEDGMENTS

The authors are grateful to the PLT technical staff for their assistance. This work was supported by the U.S. Department of Energy Contract No. DE-AC02-76-CHO-3073.

¹E. Mazzucato *et al.*, in *Proceedings of the 10th International Conference on Plasma Physics and Controlled Nuclear Fusion Research* (IAEA, London, 1984) to be published.

²R. J. Goldston, *Plasma Phys. Controlled Fusion*, **26**(1A), 165 (1984).

³K. Odajima, in *Proceedings of the 4th International Symposium on Heating in Toroidal Plasmas, Rome* (International School of Plasma Physics, EURATOM, 1984).

⁴S. Yoshikawa, M. Rothman, and R. Sinclair, *Phys. Rev. Lett.* **14**, 214 (1965).

⁵P. L. Colestock and R. J. Kashua, *Nucl. Fusion* **23**, 6 (1983).

⁶B. Stratton *et al.*, *Nucl. Fusion* **24**, 767 (1984).

⁷S. Cohen, *et al.*, *Nucl. Fusion* **24**(11), 1490 (1984).

⁸D. Manos (these proceedings).

⁹G. Hammett *et al.*, *Bull. Am. Phys. Soc.* **29**, 8 (1984).

¹⁰T. H. Stix, *Nucl. Fusion* **15**, 737 (1975).

¹¹J. Hosea, in *Proceedings of the 3rd International Symposium on Plasma Heating in Toroidal Devices* (International School of Plasma Physics, EURATOM, 1976).

¹²D. Manos *et al.*, *J. Vac. Sci. Technol. A* **2**, 1348 (1984).

¹³P. L. Colestock and R. F. Kluge, *Bull. Am. Phys. Soc.* **22**, 8 (1982).

¹⁴T. H. Stix, *Theory of Plasma Waves* (McGraw-Hill, New York, 1962), Chap. 10.

¹⁵M. Mori *et al.*, in *Proceedings of the 10th International Conference on Plasma Physics and Controlled Nuclear Fusion Research* (IAEA, London, 1984).

¹⁶F. Skiff, M. Ono, and K.-L. Wong, *Phys. Fluids* (to be published).